COSEISMIC DEFORMATIONS OF THE 2011 TOHOKU, JAPAN, EARTHQUAKE AND TRIGGERED EVENTS DERIVED FROM ALOS/PALSAR

Manabu Hashimoto[(1)], Yo Fukushima[(1)], Youichiro Takada[(1)]
[(1)] *Disaster Prevention Research Institute, Kyoto University, Gokasho, Uji, Kyoto 611-0011, Japan, hashimoto.manabu.7e@kyoto-u.ac.jp*

Abstract

The Tohoku earthquake of March 11, 2011 caused a remarkably large deformation over Honshu, Japan. By analyzing ALOS/PALSAR data, up to 3.6 m of range increase at the tip of the Oshika peninsula, the closest point to the epicenter, was detected from ascending orbits. Combining ascending and descending interferograms, this peninsula was confirmed to have subsided and shifted eastward. This deformation may have caused by huge reverse slip on the plate interface near the trench axis.

This large deformation induced activities of local earthquakes of magnitude 6 or larger, and volcanic unrests. Among them, the April 11 M7.0 event that occurred in southern Fukushima Prefecture occurred on previously unrecognized active faults. More than 9 fringes showing range increase were found in the vicinity of the epicenter of the Fukushima event. This observation is consistent with normal faulting on faults, whose motion was previously not recognized. We also found slight range increase in volcanic regions in Tohoku. These observations imply the March 11 shock induced large extensional stress in the crust of eastern Japan.

1. Introduction

The Mw9.0 Tohoku, Japan, earthquake of March 11, 2011, is the largest event during the Japanese history. Global CMT solution implies large thrust faulting on the plate interface (Fig.1), which generated huge tsunami that devastated towns on the coast and brought about ~20,000 fatalities and missing.

It is essential to reveal deformations of the Japanese Island to understand the mechanism of this extreme event in order to improve long-term forecast. A dense continuous GPS observation network (GSI's Earth Observation Network; hereafter GEONET) is deployed by the Geospatial Information Authority, Japan [e.g. Sagiya, 2004], and the coseismic deformation was immediately reported based on its data [Ozawa et al., 2011; Simons et al., 2011]. SAR Interferometry (hereafter InSAR) is another suitable technique for the detection of crustal deformation. InSAR has an advantage in its spatial resolution over GPS. After the mainshock of the Tohoku earthquake a lot of earthquakes and volcanic unrest were induced all over the eastern part of Japan. InSAR is the best to detect coseismic deformation associated with these induced events, because the size of these events is comparable to or smaller than the spacing of the network of GEONET.

Since its launch in 2006, the Advanced Land Observation Satellite (hereafter ALOS) has been conducting observation of the Earth. ALOS has a SAR sensor, the Phased Array-type L-band SAR (hereafter PALSAR). PALSAR gave us excellent data to reveal coseismic deformations such as the 2008 Wenchuan and the 2010 Haiti earthquakes [e.g. Hashimoto *et al.*, 2010; Hashimoto *et al.*, 2011]. We have been working for the Earthquake Working Group, the special project for the Evaluation of ALOS for the Disaster Mitigation, under the coordination of GSI and the Japan Aerospace Exploration Agency (hereafter JAXA), since 2007. When a large earthquake occurs, the working group requests urgent observations and analyzes acquired images. Unfortunately, ALOS terminated its operation due to a sudden power failure on April 22. It is regrettable that the PALSAR images of the Tohoku earthquake are the last message of ALOS. In this report, we show results of analyses of PALSAR images acquired before and after the 2011 Tohoku earthquake.

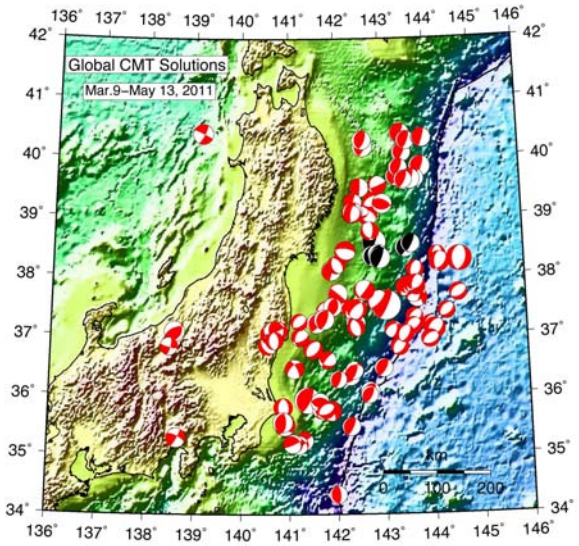

Figure 1. Distribution of CMT solutions of events (Mw>6.0) during 9 March to 13 May, 2011 [Harvard University, 2011]. Black symbols are those for foreshocks. The biggest one is for the mainshock.

Proc. 'Fringe 2011 Workshop', Frascati, Italy,
19–23 September 2011 (ESA SP-697, January 2012)

2. Acquisition of ALOS/PALSAR

PALSAR has two modes of observation useful for InSAR: strip-map and ScanSAR mode. Strip-map mode images are ~70 km wide, and have a high spatial resolution. On the other hand, ScanSAR mode images are ~350 km wide, but the spatial resolution is low. Furthermore a synchronization of bursts between two ScanSAR images is required to obtain high coherence. Therefore we requested JAXA to acquire both modes of images depending on the conditions such as the availability of archived images or conflict with other observations.

Unfortunately, power failure in ALOS occurred on April 22, and JAXA announced the completion of operation in May. Therefore we could not obtain full coverage of the eastern Japan, but the ALOS/PALSAR gave us invaluable information of the biggest earthquake in the history of Japan.

3. Image Processing

Basically strip-map mode images are acquired from the ascending orbits, while ScanSAR mode images are from descending orbits. Two strip-map mode pairs are also acquired from the descending orbits. Precise orbits are used in processing. Unfortunately the perpendicular baselines for the ScanSAR-ScanSAR pairs are longer than 2,000m, which resulted in only partially coherent interferograms. Therefore, we only show strip-map interferograms here.

We processed images with Gamma®. A hole-filed SRTM digital elevation model [Jarvis *et al.*, 2008] was used for the 2-pass differential interferometry.

4. The March 11 Mainshock

First, we discuss the deformation field observed by PALSAR. Figures 2 and 3 show the ascending and descending interferograms, respectively. We obtained high coherence in the plain area, but coherence is relatively low in the mountains. This low coherence may be attributed mainly to snow coverage.

4.1 Coseismic Interferograms

In Figure 2, we notice 30 ~ 31 cycles of fringes from the northern tip of the Shimokita peninsula (northernmost point of Honshu) to the southern tip of the Oshika peninsula for the path 401 (eastern strip). This measurement and pattern of change in color indicate range increase of about 3.5 ~ 3.6 m between these two points. Broad concentric fringes suggest that eastern the earthquake largely deformed half of the Japanese islands.

Figure 3 shows the descending interferograms. We also recognize concentric fringes whose center is located at the Oshika peninsula. The pattern of changes of color indicates range decrease. We can count 18~19

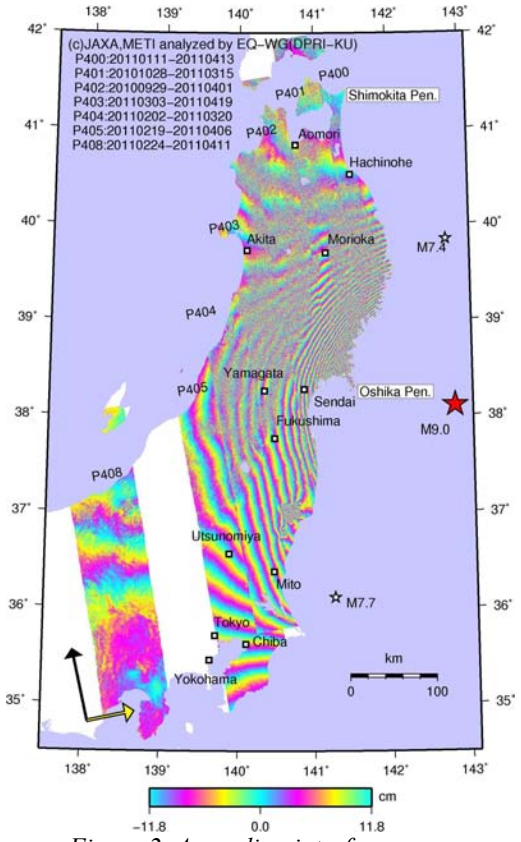

Figure 2. Ascending interferograms

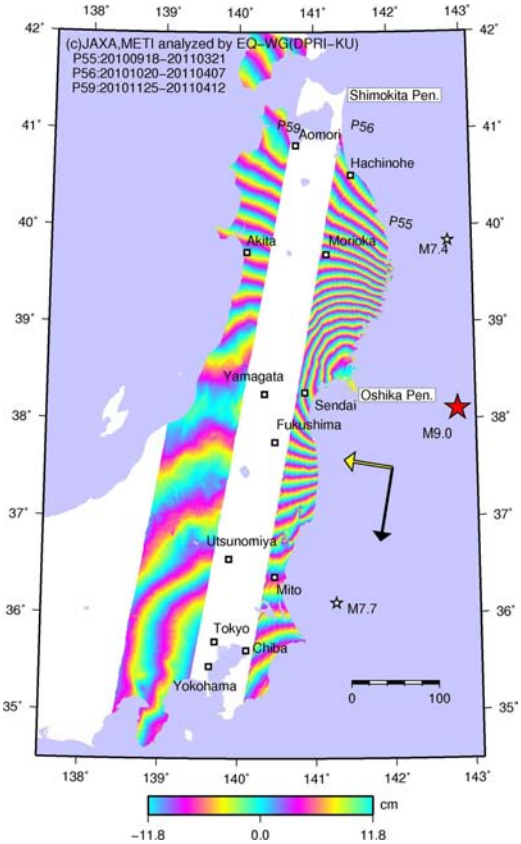

Figure 3. Descending interferograms

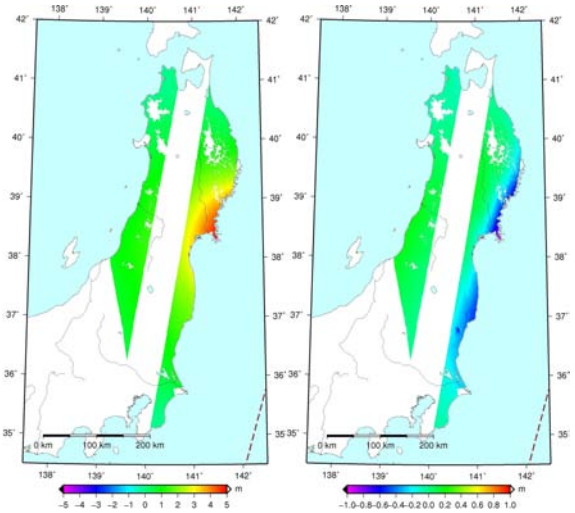

Figure 4. Result of 2.5D analysis. (left) E-W component, (right) quasi-vertical component.

cycles (2.1 ~ 2.2 m) from Hachinohe to the Oshika peninsula. It is noteworthy that the fringes are widened near the tip of the peninsula, which suggests that eastward displacement and subsidence compensate each other.

Fortunately PALSAR observed the same area from two directions. Therefore we can deduce two components of displacements. However, interferograms sometimes suffer from systematic errors possibly due to orbital inaccuracy or ionospheric disturbances. We corrected them with GPS displacements [Ozawa *et al*., 2011]. After the correction, we combined ascending and descending interferograms to obtain east-west and quasi-vertical components (Figure 4). We found ~5 m eastward shift of the Oshika peninsula and ~1 m subsidence along the Pacific coast of the entire eastern Japan.

4.2 Slip Distribution

In order to understand the mechanism of this gigantic earthquake, we performed an inversion of slip distribution using the algorithm proposed by Fukahata and Wright (2008). We assumed a single fault plane dipping toward west from the trench axis with a 600 km length. In this inversion, we simultaneously estimated dip angle of the fault plane. We also assumed the depth range of fault is 100 km. Only dip slip components of slip were estimated. Since we have data only on the west side of the source, a preliminary inversion found that it is very hard to estimate the strike-slip component simultaneously with the dip-slip component.

So far we searched an optimal dip angle in a range from 10 to 20 degree and found 20 degree gives the minimum ABIC (Akaike's Bayesian Information Criterion). Though there is a possibility that more steep dip angles give better results, we adopted this value since the nodal plane of CMT solution has a shallow dip angle. Furthermore, a model with higher variable slip distribution can explain the data better, but we prefer relatively smoother solution. It is because there are no data above the source area and data on land have no resolving power of slip. Therefore we selected solution with seismic moment consistent with GCMT (Figures 5 and 6).

The peak of slip of ~50 m is located between the epicenter and trench axis. This model is roughly consistent with that of Simons *et al.*(2011) obtained from GPS, tsunami and seismic data. Synthetic interferogams are consistent with the observed ones.

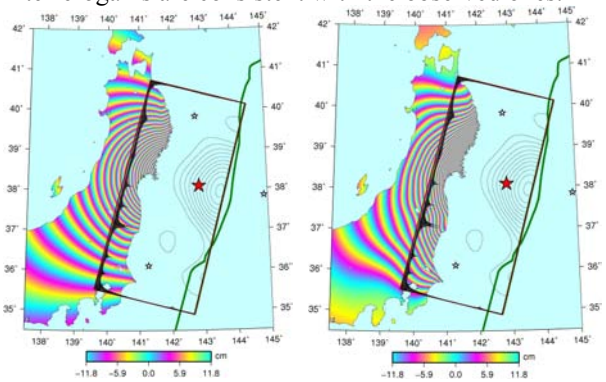

Figure 5. Synthetic interferograms. (left) Descending, (right) Ascending. Rectangle indicates surface projection of modeled fault plane. Slip contours of 5m are also shown. Star is the epicenter of the mainshock.

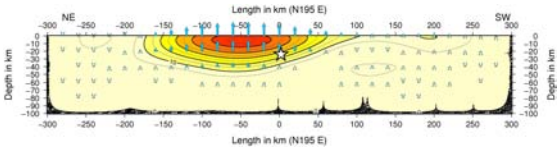

Figure 6. Slip distribution projected onto the vertical cross section along the strike of modeled fault

5. Triggered Events

In Figures 2 and 3, we notice several local disturbances. These are deformations due to induced earthquakes, volcanic unrests and possible landslides. Figure 7 shows the residual interferograms of the previous inversion. Local disturbances are more clearly recognized.

5.1 The April 11 Fukushima Earthquake

The most prominent signal of induced activities is found north of Mito. Since March 19, seismic swarm including a couple of M>6 events occurred in southern Fukushima and northern Ibaraki prefectures. On April 11, the largest event with Mw6.6 occurred and its aftershock activity still continues. Since the hypocenters of these induced earthquakes are shallow, InSAR detected coseismic deformation. Figure 8 shows a close-up of its source area in an ascending interferogram (Path 403). We can count more than 18

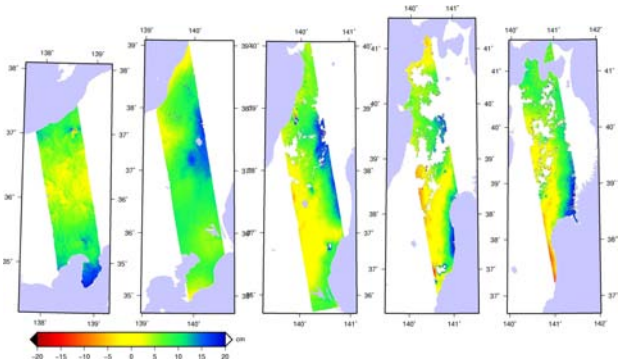

Figure 7(a). Residuals the inversion in ascending interferograms from path 408 (left) to 402(right).

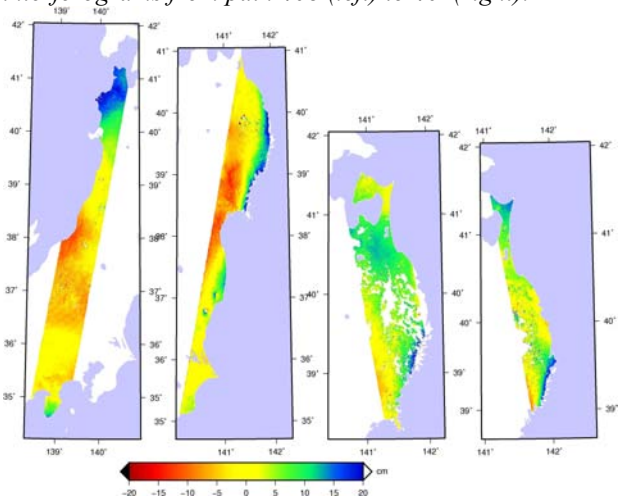

Figure 7(a). Residuals the inversion in descending (left: path 59 and 56) and ascending interferograms (right: path 401 and 400).

fringes (>2.1 m) there. Discontinuities of fringes correspond well to the surface ruptures [Ishiyama et al., 2011]. The pattern of change of color implies range increase and its peak is located on the west side of the faults. Since the normal faulting mechanism was observed, the western blocks are on hanging wall side. Interestingly, the peak is located in mountain ranges, while the central part between reverse V-shaped faults is a valley. These observations are inconsistent with local topography. This area has not experienced large earthquake in its history. Therefore we think old faults were reactivated by large extensional stress due to the 11 March mainshock.

5.2 Local Disturbances in Interferograms

We recognized other local disturbances due to earthquakes larger than Mw6 (Mw6.3 Northern Nagao earthquake of March 11 and other event in southern Fukushima and northern Ibaraki areas). However there are several local disturbances that may not be accompanied by significant earthquakes. In the residual interferograms of paths 402 and 403, tiny green spots can be seen north of Sendai (Figure 7a). Figure 9 is close-up of original interferogram of path 402. We have elliptical fringes of one cycle west of Hanayama Lake and near Mt. Kurikoma. The former might be related to activity of landslide, while the latter might be related to volcanic activity.

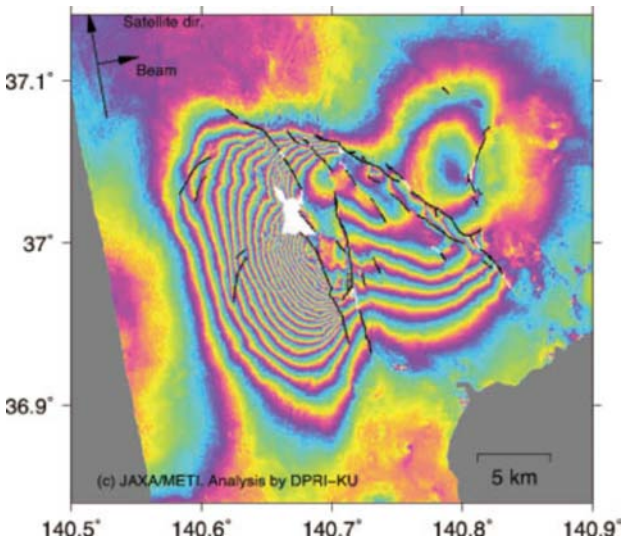

Figure 8. Close-up of interferogram in the epicentral area of the 11 April Southern Fukushima earthquake (Mw6.6). Solid lines are recognized traces of faults.

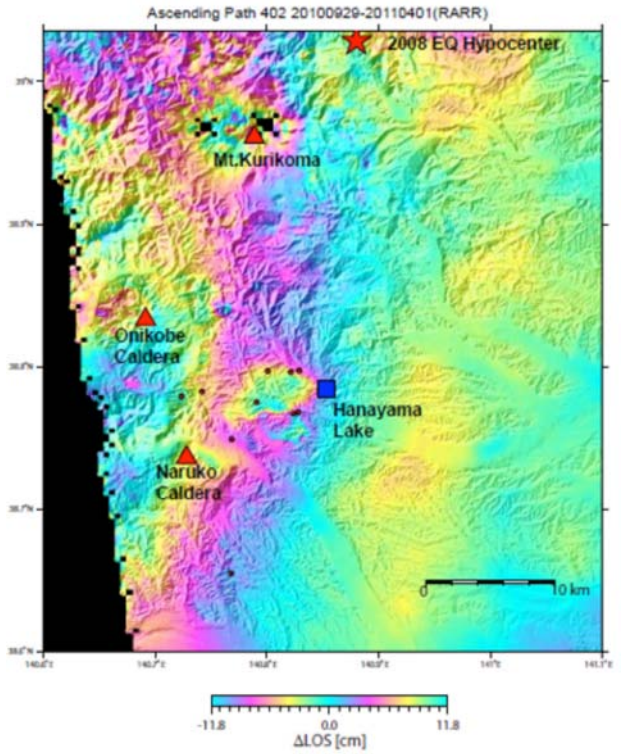

Figure 9. Close-up of interferogram of the path 402. Two elliptical fringes are recognized near Hanayama Lake and Mt. Kurikoma.

6. Summary

We found very large deformation due to the 11 March main shock and local deformations due to induced earthquakes using ALOS/PALSAR images. PALSAR images suggest huge slip on the interface between plates near the trench axis. We also found other local deformations near volcanoes or possible landslides. Especially, 11 April Southern Fukushima earthquake caused deformation that is inconsistent with local topography. We are going to deduce characteristics of these deformations and understand its mechanism.

Unfortunately, ALOS/PALSAR completed its operation in May. JAXA is preparing the next L-band SAR mission. We believe the next mission, ALOS-2, will definitely contribute to the earthquake science.

ACKNOWLEDGEMENTS

PALSAR level 1.0 data are shared among PIXEL (PALSAR Interferometry Consortium to Study our Evolving Land Surface), and provided from JAXA under cooperative research contract with ERI, Univ. Tokyo, and the Earthquake Working Group (Geospatial Information Authority) under the JAXA's project "Utilization of ALOS for Disaster Mitigation". The ownership of PALSAR data belongs to METI (Ministry of Economy, Trade and Industry) and JAXA.

REFERENCES

Harvard University Global CMT Project: http://www.globalcmt.org/, 2011.

Hashimoto, M., M. Enomoto, and Y. Fukushima, Coseismic Deformation from the 2008 Wenchuan, China, Earthquake Derived from ALOS/PALSAR Images, *Tectonophysics*, **491**,59-71, 2010.

Hashimoto, M., Y. Fukushima, and Y. Fukahata, Fan delta uplift and mountain subsidence during the 2010 Haiti earthquake, *Nature Geoscience*, 4, 255-259, doi:10.1038/ngeo1115, 2011.

Ishiyama, T., H. Sato, T. Ito, N. Sugito, T. Echigo, N. Kato, and T. Imaizumi, The surface earthquake fault of the 11th April 2011 earthquake in Hamadoori Fukushima pref., http://outreach.eri.u-tokyo.ac.jp/eqvolc/201103_tohoku/eng/hamadoori/, 2011.

Jarvis, A., Reuter, H.I., Nelson, A. & Guevara, E. Hole-filled SRTM data V4. International Centre for Tropical Agriculture (CIAT), http://www.srtm.csi.cgiar.org, 2008.

Ozawa, S., T. Nishimura, H. Suito, T. Kobayashi, M. Tobita, and T. Imakiire, Coseismic and postseismic slip of the 2011 magnitude-9 Tohoku-Oki earthquake, Nature, doi:10.1038/nature10227, 2011.

Sagiya, T., A decade of GEONET: 1994-2003 - The continuous GPS observation in Japan and its impact on earthquake studies -, *Earth Planets Space*, **56**, xxix-xli, 2004.

Simons, M., *et al.*, The 2011 magnitude 9.0 Tohoku-Oki earthquake: mosaicking the megathrust from seconds to century, *Science*, **332**, 1421, doi:10.1126/science.1206731, 2011.